

From the Monsanto Company, St. Louis, Missouri (U.S.A.)

Morphology and the elastic modulus of block polymers and polyblends

By L. E. Nielsen*)

With 7 figures and 1 table

(Received October 27, 1972)

Introduction

The elastic moduli and morphology of block polymers and polyblends can be modified by changing the relative concentration of the components, by heat and solvent treatments, and by the intensity of mechanical mixing. In these two-phase systems the dispersed phase can be spheres, aggregated spheres, or cylindrical or plate-like in shape. Over certain composition ranges, both phases can be continuous, or the phases can become inverted- the dispersed phase can become the continuous phase. These different morphologies have widely different moduli and other mechanical properties. It will be shown that if the morphology of a given block polymer or polyblend is known, then reasonable predictions of the elastic moduli can be made by using the theoretical equations developed for composite materials.

Theory

Earlier attempts to relate the concentration of the two components and the morphology of two phase systems such as polyblends and block polymers with their elastic moduli have been made by *Takayanagi* (1, 2) and by *Kaelble* (3, 4). These workers used series and parallel combinations of the components in models which give the highest upper bound and the lowest lower bound to the modulus. It is very difficult to relate the modulus of such a model with the actual morphology of the real system.

A better method which imposes much narrower limits on the moduli and which is capable of incorporating the morphology of the two-phase system in a less ambiguous manner is to use the recent theory of the moduli of composite materials. *Kerner* (5) developed a theory in which either of the phases can be a dispersion of spheres in a matrix of the other component. More recently *Halpin* and *Tsai* (6, 7) have developed

equations which are general enough to cover the complete range of moduli from the lowest lower bound (series models) to the highest upper bound (parallel models). They also showed how the moduli can be calculated for many systems of widely different morphologies including dispersions of spheres, fiber-filled materials, etc. *Nielsen* (8) extended the *Halpin-Tsai* equations by using the concept of a generalized *Einstein* coefficient to cover still other morphologies, including dispersions of aggregated spheres and short fibers randomly oriented. *Lewis* and *Nielsen* (9, 10) were able to narrow the limits on the upper and lower bounds on the moduli by taking into account the maximum packing fraction of the filler phase.

The highest upper bound of the modulus is given by the rule of mixtures:

$$M = M_1 \varphi_1 + M_2 \varphi_2 \quad [1]$$

where M is the modulus of the composite, M_1 is the modulus of component 1, and φ_1 is the volume fraction of component 1. This equation holds for models in which the components are arranged parallel to one another so that an applied stress elongates each component the same amount. The lowest lower bound to the modulus is found in models in which the components are arranged in series with the applied stress; the equation for this case is:

$$\frac{1}{M} = \frac{\varphi_1}{M_1} + \frac{\varphi_2}{M_2} \quad [2]$$

Curves numbered 1 and 2 of fig. 1 for the modulus of the composite divided by the modulus of the rubber correspond to eqs. [1] and [2] for the case of $M_2/M_1 = 1000$. This modulus ratio is approximately the correct value for composites made up of a rigid polymer and an elastomer.

*) HPC71-144 from the Monsanto/Washington University Association sponsored by the Advanced Research Projects Agency, Department of Defense, under Office of Naval Research Contract N00014-67-C-0218.

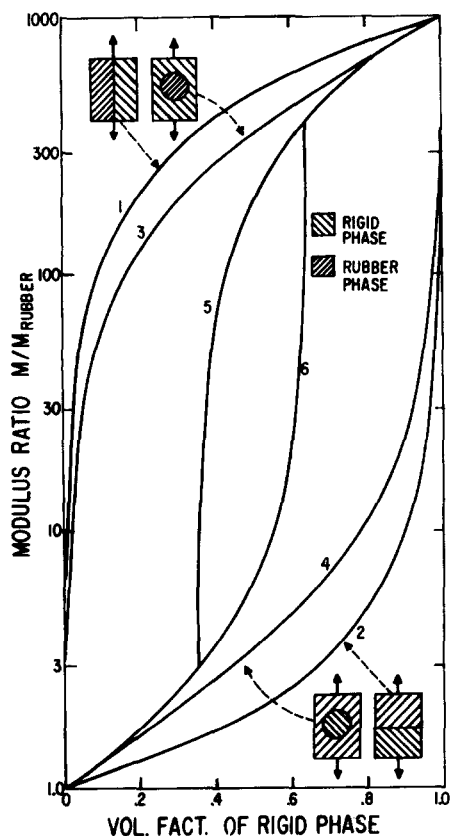


Fig. 1. Modulus ratio of composites. Curve 1: parallel element model; curve 2: series model; curve 3: *Halpin-Tsai* (or *Kerner*) shear modulus for elastomeric spheres dispersed in a rigid polymer; curve 4: rigid spheres dispersed in elastomeric phase; curve 5: elastomeric spheres in rigid matrix for $\phi'_m = 0.64$ (random packing); and curve 6: rigid spheres dispersed in an elastomeric matrix for $\phi_m = 0.64$

The *Halpin-Tsai* equations are (6, 7):

$$\frac{M}{M_1} = \frac{1 + AB\phi_2}{1 - B\phi_2} \quad [3]$$

$$B = \frac{M_2/M_1 - 1}{M_2/M_1 + A} \quad [4]$$

where the subscripts 1 and 2 refer to the continuous phase and the dispersed phase, respectively. The constant A is determined by the morphology of the system; for dispersed spheres in an elastomeric matrix, $A = 1.5$, for instance. The extension of these equations is given by (8–10):

$$\frac{M}{M} = \frac{1 + AB\phi_2}{1 - B\psi\phi_2} \quad [5]$$

$$A = k - 1 \quad [6]$$

$$\psi = 1 + \frac{(1 - \phi_m)}{\phi_m^2} \phi_2 \quad [7]$$

where k is a generalized *Einstein* coefficient, and ψ is a function which takes into account the maximum packing fraction ϕ_m of the dispersed phase. The maximum volumetric packing fraction ϕ_m is indirectly related to morphology, and it generally has a value between 0.5 and 0.9. It has a value of 1.0 in the original *Halpin-Tsai* equations. The constants A and k are strongly dependent upon the morphology of the composite.

For inverted systems in which the continuous phase is the more rigid one, it is convenient to rewrite equations 4–6 as

$$\frac{M_1}{M} = \frac{1 + A_i B_i \phi_2}{1 - B_i \psi \phi_2} \quad [8]$$

$$B_i = \frac{M_1/M_2 - 1}{M_1/M_2 + A_i} \quad [9]$$

and

$$A_i = \frac{1}{A}. \quad [10]$$

In the inverted system, the subscript 2 still refers to the dispersed phase, which is now the low modulus phase.

Curves 3 and 4 of fig. 1 illustrate the *Halpin-Tsai* equations for dispersed spheres. Curves 5 and 6 of fig. 1 illustrate the modified eqs. [5]–[10] for dispersed spheres with $\phi_m = 0.64$ (random close packing), a *Poissons* ratio of 0.5 for the elastomer phase, and a *Poissons* ratio of 0.35 for the rigid phase. The *Halpin-Tsai* equations and their modification put much narrower limits on the moduli than the series or parallel models used in the past. Morphologies other than dispersed spheres generally have similar spreads between the upper and lower modulus curves.

In real systems of polyblends and block polymers, both phases may be continuous, or there may be an inversion of the phases as the composition ratio is changed. In this situation the equations giving the upper and lower bounds to the modulus must be combined in some manner. Empirically it has been known for a long time, and recent calculations on crystalline polymers (11) indicate, that a combination of the two equations is approximately given by

$$\log M = \phi_u \log M_u + \phi_L \log M_L. \quad [11]$$

M_u and M_L are the upper and lower bounds to the modulus, respectively, at a given composition. In this equation ϕ_u is the fraction of the low

modulus material that is in a continuous phase in the overlap region where both phases are essentially continuous, while φ_L is the fraction of the rigid material that is in the overlap region (10).

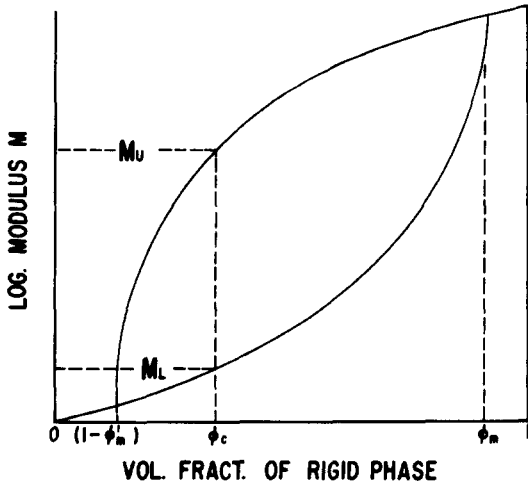


Fig. 2. Notation used in calculation of modulus when there are two continuous phases over part of the composition range

Fig. 2 may illustrate the point more clearly for some chosen over-all composition φ_c .

$$\varphi_L = \frac{\varphi_c - (1 - \varphi'_m)}{\varphi_m - (1 - \varphi'_m)} \quad [12]$$

$$\varphi_u = 1 - \varphi_L = \frac{\varphi_m - \varphi_c}{\varphi_m - (1 - \varphi'_m)} \quad [13]$$

φ'_m is the packing fraction of the low modulus material in the inverted system. For the unmodified Halpin-Tsai equations, φ_L is the volume fraction of the rigid phase, and φ_u is the volume fraction of the elastomeric phase for any value of φ_c .

The Einstein coefficient k (or A), which is very sensitive to the morphology of the system, is proportional to the initial slope of the modulus-concentration curve near $\varphi = 0$ and $\varphi = 1$ for dispersed systems in which both phases are not continuous. Einstein coefficients have been published for many systems (6, 12, 13). Some of these are listed in table 1. The listed values of k [or of $(A + 1)$] are for rigid particles in a matrix of lower modulus. The values for inverted systems, in which the matrix has a higher modulus than the dispersed phase, can be determined from eqs. [6] and [10]. If Poissons ratio of the matrix is not 0.5, a correction should be applied to the Einstein coefficient (8).

Table 1. Einstein coefficients for composites

| Filler phase | Modulus | Einstein coefficient k |
|---|----------|----------------------------------|
| Spheres | G | $1 + (7 - 5\nu_1)/(8 - 10\nu_1)$ |
| Large aggregates of spheres | G | $2.50/\varphi_a$ |
| Aggregates of 2 spheres | G | $2.58 +$ |
| Rods-axial ratio 4 | G | 3.08 |
| Rods-axial ratio 6 | G | 3.84 |
| Rods-axial ratio 8 | G | 4.80 |
| Rods-axial ratio 10 | G | 5.93 |
| Rods-axial ratio 15 | G | 9.4 |
| Uniaxial fiber-filled | E_L | $1 + 2L/D$ |
| Uniaxial fiber-filled | E_T | 1.5 |
| Uniaxial fiber-filled | G_{LT} | 2.0 |
| Uniaxial fiber-filled | G_T | 1.5 |
| Ribbon-filled ($w/t \rightarrow \infty$) | E_L | ∞ |
| Ribbon-filled | E_T | $1 + 2w/t$ |
| Ribbon-filled | E_{TT} | 1.0 |
| Ribbon-filled | G_{LT} | $1 + (w/t)$ (13) |
| Ribbon-filled ($w/t \rightarrow \infty$) | G_{LT} | 1.0 |
| Ribbon-filled ($w/t \rightarrow \infty$) | G_{TT} | 1.0 |
| $M = M_1\varphi_1 + M_2\varphi_2$ | M | ∞ |
| $\frac{1}{M} = \frac{\varphi_1}{M_1} + \frac{\varphi_2}{M_2}$ | M | 1.0 |

| | |
|---------------|--|
| ν_1 | Poissons ratio of matrix |
| φ_a | Packing fraction of spheres in aggregate |
| L | Length of rod |
| D | Diameter of rod |
| w | Width of ribbon |
| t | Thickness of ribbon |
| T | Transverse to fibers or ribbons |
| Subscript L | Longitudinal direction |

The values of the Einstein coefficient or of A do not uniquely define the morphology of a system; more than one kind of morphology can have the same Einstein coefficient. For instance, aggregates of spheres can have the same values as short fibers or rods. In addition, some phases may appear to be continuous when they actually are not. For instance, very long, but discontinuous, fibers, ribbons, and oriented flakes may give high moduli characteristic of a continuous phase. Thus, if one or more of the dimensions of a particle are very large compared to the other dimensions, such fillers appear to the matrix phase to be continuous. Therefore, moduli do not completely describe a system; additional morphological information is required. However, on the other hand, if the morphology of a system is known, in principle the moduli can be accurately calculated. In the overlap region where both phases are essentially continuous, the exact morphology does not appear to be important.

The important factor is then how much of each phase is present, and this is determined by φ_m and φ'_m . Changes in morphology which occur as the concentration changes are also largely compensated for by the values of φ_m and φ'_m since they depend upon the packing and morphology at high concentrations while the value of the *Einstein* coefficient is determined by the morphology at very low concentrations.

Experimental

Four examples from the literature will be used to illustrate the use of the theory. The first example is a series of styrene-butadiene-styrene block polymers reported by Holden et al. (14) and discussed by Kaelble (3, 4). Fig. 3 shows the experimental data for Young's modulus and a calculated curve which fits the data quite well.

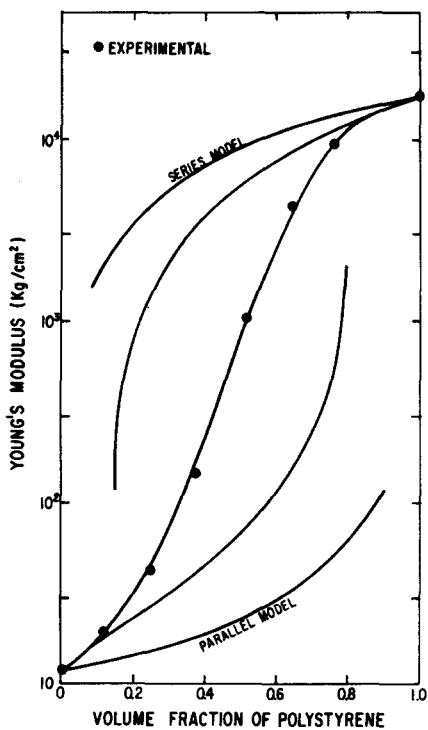


Fig. 3. Modulus of S-BD-S block polymers as a function of composition. Center curve calculated using $A = 3.0$, $\varphi_m = 0.80$, $v_1 = 0.5$, $A_i = 0.86$, $\varphi'_m = 0.85$, $v_1 = 0.35$

The calculated curve results from two curves using the following values: 1. Polystyrene dispersed in polybutadiene with $A = 3.0$ and $\varphi_m = 0.8$. 2. Polybutadiene dispersed in polystyrene with $A_i = 0.86$, $\varphi'_m = 0.85$, and a polystyrene *Poissons* ratio of 0.35. (A better fit to the data might be obtained by changing these

values somewhat, but these illustrate the point.) Unfortunately, the morphology of these samples has not been published, but the above values strongly suggest the following changes in morphology as the concentration of polystyrene increases: At low concentrations of polystyrene, the polystyrene appears to be either aggregates of about six spheres (13) or rods with an aspect ratio of about 6 to 1.0 (12). Already at about 15% polystyrene, both phases tend to be continuous. The region of phase inversion where both phases are more or less continuous covers the range from 15–80% polystyrene. From 80–100% polystyrene, the polybutadiene is dispersed as spheres in the polystyrene. This type of information would be hard to deduce from series or parallel models, the limits of which are also shown in fig. 3. However, as pointed out by Kaelble, such models do also predict phase inversion for this series of block polymers.

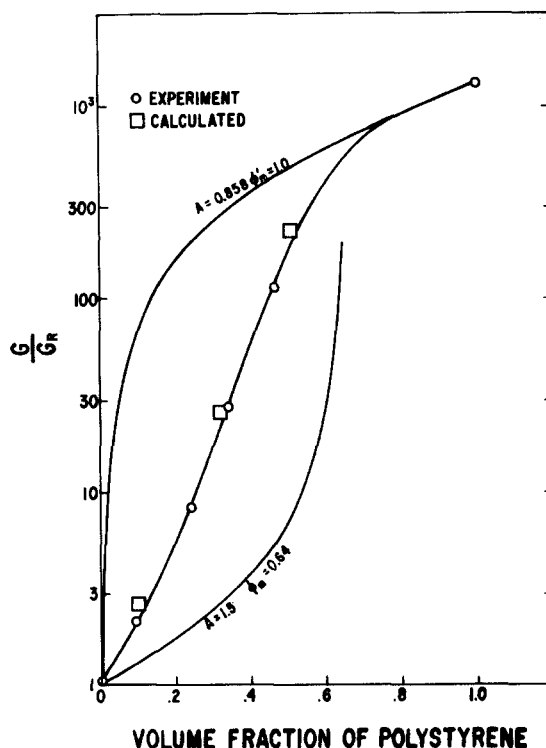


Fig. 4. Modulus of polyblends of polystyrene and SBR

A second example is a series of polyblends of polystyrene in styrene-butadiene rubber as reported by Kraus et al. (15). Fig. 4 shows the experimental values along with calculated values using the following constants: $A = 1.5$, $\varphi_m = 0.64$, $A_i = 0.86$, $\varphi'_m = 1.0$, and *Poissons* ratios of 0.5 and 0.35 for the rubber and the polystyrene,

respectively. Again, the detailed morphology of these materials has not been published, but the above constants suggest the following behavior on addition of polystyrene to rubber: Almost immediately at very low concentrations of polystyrene, it tends to become a continuous phase, possibly by forming fibrous strings with an aspect ratio of about 15 to 1.0. The region of two continuous phases continues until a volume fraction of about 0.64 is reached. At higher concentrations of polystyrene, the rubber appears to be dispersed as spheres, although there are no experimental points except the point for pure polystyrene to really make this conclusion valid. In any case, the morphology is such as to make the experimental curve unsymmetrical about the mid composition point of $\phi = 0.5$. On the other hand, the block polymer case is nearly symmetrical about $\phi = 0.5$.

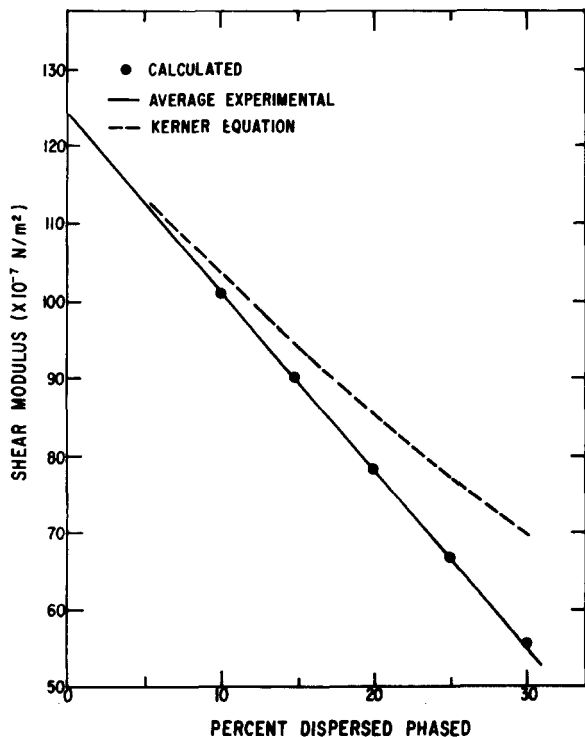


Fig. 5. Modulus of polystyrene containing a dispersed elastomeric phase. The solid line is the average experimental modulus line of *Cigna*. The points were calculated using $A_i = 0.86$ (spheres), $\phi'_m = 0.55$, and $v_1 = 0.35$

The third example is a series of polystyrene-elastomer blends studied by *Cigna* (16). Electron microscopy showed these materials to be essentially spheres of the elastomers in a polystyrene matrix with little, if any, tendency for phase inversion to occur at concentrations of elastomers

below 30%. Many polyblends were studied, undoubtedly with small changes in morphology, so at a given concentration of elastomer there was some scatter in the values of the shear moduli. An average experimental curve was drawn by *Cigna* through the experimental points as shown in fig. 5. The *Kerner* equation (or the *Halpin-Tsai* equation for spheres) gave values considerably higher than the experimental values. However, the modified equations using $\phi'_m = 0.55$ and $A_i = 0.86$ gave good agreement with the experimental values. A value of $A_i = 0.86$ is the expected value for spheres in a matrix of *Poissons* ratio 0.35. A value of $\phi'_m = 0.55$ is between the values for random loose packing (0.60) and simple cubic packing (0.524) of spheres. Thus, in this case the behavior predicted from the morphology is in very good agreement with the actually observed experimental results.

An example where the discontinuous phase does not appear to be dispersed spheres at either end of the composition range is the series of polyblends of polybutadiene and styrene-butadiene (SBR) rubber reported by *Fujimoto et al.* (17). The SBR copolymer contained 57.3% styrene. A comparison of the experimental data at 25 °C and the calculated results are given in fig. 6. An

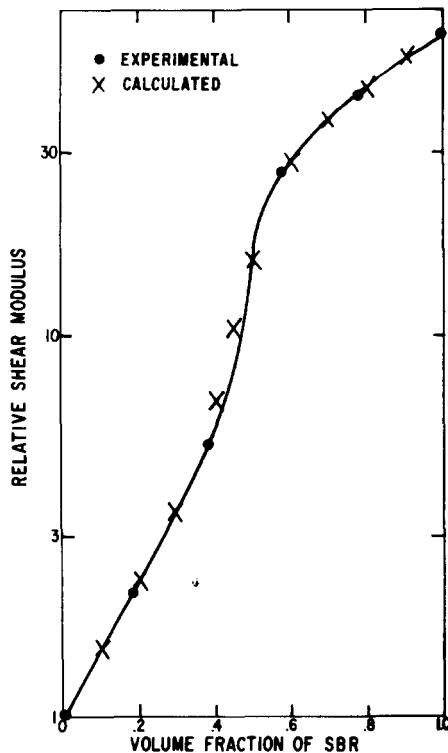


Fig. 6. Modulus of polybutadiene - SBR rubber blends at -25 °C

excellent match of the experimental results is achieved by using the values: $A = 4.35$, $B = 0.92$, $\varphi_m = 0.60$, $A_i = 0.3$, $B_i = 0.97$, $\varphi'_m = 0.70$. The *Einstein* coefficients (or A values) indicate that the dispersed phases near $\varphi \approx 0$ and $\varphi \approx 1$ are not dispersed spheres but are either fibers with an average aspect ratio of about 8 to 1 or very large aggregates. This system also has a very narrow range of compositions in which two continuous phases simultaneously exist; phase inversion is complete between a volume fraction of 0.3–0.6 of SBR copolymer.

Where the necessary morphological information is available in the four examples discussed, there is agreement between the experimental and the calculated results. In the other cases, reasonable morphologies have been deduced by fitting the theoretical equations to the experimental data. However, additional information on the morphology is needed to test the complete validity of this approach.

Acknowledgment

This research was supported by the Advanced Research Projects Agency of the Department of Defense and was monitored by the Office of Naval Research under Contract No. N00014-67-C-0218.

Appendix

Justification for the logarithmic rule of mixtures in the overlap region

Empirically, it has been known that the logarithmic rule of mixtures (eq. [11]) is useful for predicting the modulus of crystalline polymers as a function of the degree of crystallinity or for predicting the modulus of polyblends in the region of phase inversion. Very little theoretical justification for its use has been presented, however. There are two intuitive arguments for its use:

1. There are two general equations which are capable of covering all values of the moduli M of composite systems from the lowest lower bound to the greatest upper bound. These are the *Halpin-Tsai* equations (eqs. [3]–[5]), and

$$M^n = M_1^n \varphi_1 + M_2^n \varphi_2; \quad -1 \leq n \leq +1. \quad [a]$$

The logarithmic rule of mixtures is the limiting case of eq. [a] as $n \rightarrow 0$. The *Halpin-Tsai* equations and eq. [a] are symmetrical with respect to all upper and lower bounds when $\log M$ is plotted as a function of φ_2 . They are not symmetrical on a M versus φ_2 plot.

2. The second argument involves giving equal relative weighting factors to both low and high moduli. When the upper and lower limits to the moduli are greatly different, equal weighting is achieved on a logarithmic scale but not on a linear scale.

The most important argument for using a logarithmic rule of mixtures can be visualized by writing eq. [11] in exponential form

$$M = M_U^\varphi \cdot M_L^{\varphi_L} \quad [b]$$

where subscripts U and L refer to equations for the upper and lower bounds of the moduli. The quantities φ_L and φ_U refer to the relative amount of each phase participating as a continuous phase—not the total amount of each phase present. Thus, φ_L can be considered the “connectivity” of the rigid phase. If $\varphi_L = 0$, none of the rigid phase is continuous, while if $\varphi_L = 1$, all of the rigid phase is continuous in the region of overlap between $(1 - \varphi'_m)$ and φ_m (see fig. 2). Likewise, φ_U can be considered the “connectivity” of the low modulus component in the overlap region. The concept of connectivity can be illustrated by the overly simplified sketches in fig. 7. In fig. 7A and 7C, the rubber phase is dispersed (its connectivity is zero), and the modulus of the composite is high. In fig. 7B and 7D the connectivity φ_U has increased, and the modulus of the composite decreases even though the quantity of rubber has not changed and the appearance of the rubber phase is nearly the same. A similar, but inverse situation, holds if $G_1 > G_2$ so that the connectivity φ_L of the rigid component increases in going from fig. 7A to 7B. As the connectivity of one phase increases, the connectivity of the other phase decreases in accordance with the equation

$$\varphi_L + \varphi_U = 1. \quad [c]$$

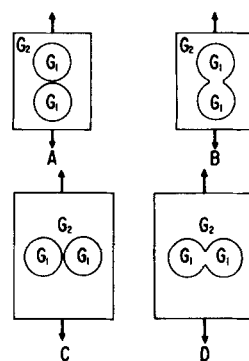


Fig. 7. Schematic diagrams illustrating the concept of connectivity of phases. Phase 1 has zero connectivity in A and C

In the overlap region where phase inversion is taking place, the connectivities φ_L and φ_U change more rapidly than the volume fractions of the components φ_1 and φ_2 .

The connectivity must be random in nature for the logarithmic rule of mixtures to hold. If the connectivity of the particles becomes oriented primarily in one direction, anisotropy develops. In the extreme case of orientation parallel to the direction of stress, a parallel type of model holds in which the ordinary rule of mixtures is obeyed:

$$M = M_1 \varphi_1 + M_2 \varphi_2. \quad [d]$$

The other extreme is orientation perpendicular to the direction of applied tensile stress; in this case a series type of model system develops in which the inverse rule of mixtures holds:

$$\frac{1}{M} = \frac{\varphi_1}{M_1} + \frac{\varphi_2}{M_2}. \quad [e]$$

On a log M versus φ_2 plot, eqs. $[\eta]$ and $[\epsilon]$ are symmetrical about the line for the logarithmic rule of mixtures. Rotation of such plots 180° corresponds to rotating the specimen 90° .

Summary

The theory of the elastic moduli of composite materials in which an inversion of the phases can occur is reviewed. The morphology of the system and the packing fraction of the dispersed phase are important in determining the moduli. The applicability of the theoretical equations is illustrated for four systems of block polymers and polyblends. In three of the systems, phase inversion occurs. Agreement between theory and experiment is good, and where the morphology of the composites is known, the moduli agree with the values expected for that morphology.

Zusammenfassung

Die Elastizitätsmodul-Theorie der zusammengesetzten Stoffe, in welchen eine Phaseninversion vorkommen kann, wird untersucht. Die Systemmorphologie und die Packungsfraction der dispersen Phase sind für die Modulbestimmung wichtig. Die Anwendbarkeit der theoretischen Gleichungen ist für vier Systeme von Blockpolymeren und Polygemischen veranschaulicht. Eine Phaseninversion kommt in drei von den Systemen vor. Die Theorie und Praxis sind in einer guten Übereinstimmung, und da, wo die Morphologie der zusammengesetzten Stoffe bekannt ist, stimmen die Moduli mit den für die Morphologie erwarteten Werten überein.

References

1) *Takayanagi, M.*, Proc. 4th Internat. Congr. Rheol., Part 1, p. 161, *Lee and Copley* (Ed.) (New York 1965).

- 2) *Manabe, S., R. Murakami, and M. Takayanagi*, Memoirs Faculty of Eng. Kyushu Univ. **28**, 295 (1969).
- 3) *Kaelble, D. H.*, Physical Chemistry of Adhesion, p. 415 (New York 1971).
- 4) *Kaelble, D. H.*, Trans. Soc. Rheol. **15**, 235 (1971).
- 5) *Kerner, E. H.*, Proc. Phys. Soc. **B 69**, 808 (1956).
- 6) *Ashton, J. E., J. C. Halpin, and P. H. Petit*, Primer on Composite Analysis, Chap. 5 (Stamford, Conn., (1969).
- 7) *Halpin, J. C.*, J. Compos. Mater. **3**, 732 (1969).
- 8) *Nielsen, L. E.*, J. Appl. Phys. **41**, 4626 (1970).
- 9) *Lewis, T. B. and L. E. Nielsen*, J. Appl. Polym. Sci. **14**, 1449 (1970).
- 10) *Nielsen, L. E.*, Appl. Polym. Symp., No. 12, 249 (1969).
- 11) *Gray, R. W. and N. G. McCrum*, J. Pol. Sci., Part A 2, **7**, 1329 (1969).
- 12) *Burgers, J. M.*, Second Report on Viscosity and Plasticity, p. 113 (New York 1938).
- 13) *Lewis, T. B. and L. E. Nielsen*, Trans. Soc. Rheol. **12**, 421 (1968).
- 14) *Holden, G., E. T. Bishop, and N. R. Legge*, J. Polym. Sci. **C 26**, 37 (1969).
- 15) *Kraus, G., K. W. Rollmann, and J. T. Gruver*, Macromol. **3**, 92 (1970).
- 16) *Cigna, G.*, J. Appl. Polym. Sci. **14**, 1781 (1970).
- 17) *Fujimoto, K. and N. Yoshimura*, Rubber Chem. Tech. **41**, 1109 (1968).

Author's address:

Dr. Lawrence E. Nielsen
Monsanto Company
800 N Lindbergh
St. Louis, Missouri, 63166 (USA)